Optical field enhancement in nanoscale slot waveguides of hyperbolic metamaterials

Yingran He,[1,2] Sailing He,[2] and Xiaodong Yang[1,*]

[1]*Department of Mechanical and Aerospace Engineering, Missouri University of Science and Technology, Rolla, Missouri 65409, USA*

[2]*Centre for Optical and Electromagnetic Research, Zhejiang Provincial Key Laboratory for Sensing Technologies, Zhejiang University, Hangzhou 310058, China*

*Corresponding author: yangxia@mst.edu

Nanoscale slot waveguides of hyperbolic metamaterials are proposed and demonstrated for achieving large optical field enhancement. The dependence of the enhanced electric field within the air slot on waveguide mode coupling and permittivity tensors of hyperbolic metamaterials is analyzed both numerically and analytically. Optical intensity in the metamaterial slot waveguide can be more than 25 times stronger than that in a conventional silicon slot waveguide, due to tight optical mode confinement enabled by the ultrahigh refractive indices supported in hyperbolic metamaterials. The electric field enhancement effects are also verified with the realistic metal-dielectric multilayer waveguide structure. © 2012 Optical Society of America

OCIS codes: 130.3120, 230.7370, 160.3918.

It was proposed that considerable electric field enhancement will occur at the low-index slot region of coupled high-index waveguides, as a result of the normal electric displacement continuity at the high-index-contrast interface implemented by Maxwell's equations [1]. Silicon slot waveguides are attractive, as silicon can provide a high refractive index ($n_{si} = 3.48$ at 1.55 μm) and thus a large field enhancement [2]. For further boost of the optical field inside the low-index slot region, a material with a higher refractive index is preferable. Although high indices of refraction at optical frequencies are not available in natural materials, metamaterials with artificially engineered unit cells can be carefully designed to achieve this goal [3,4]. Particularly, hyperbolic metamaterials with extreme anisotropy, in which not all the principal components of the permittivity tensor have the same sign, can support large wave vectors and therefore ultrahigh effective refractive indices [5–9].

In this Letter, we will present a new type of slot waveguide made of hyperbolic metamaterials with ultrahigh refractive indices, where the optical field within the slot region can be significantly enhanced. The dependences of the electric field enhancement on gap sizes between two coupled waveguides and permittivity tensors of hyperbolic metamaterials are systematically studied with numerical simulation and theoretical analysis. It is demonstrated that the maximum optical intensity in the slot waveguides of hyperbolic metamaterial can be more than 25 times stronger than that in a silicon slot waveguide, due to the ultrahigh refractive indices in hyperbolic metamaterials. The metamaterial slot waveguides with extremely tight photon confinement will be important in enhanced light–matter interactions, such as nonlinear optics [10], optomechanics [11], and quantum electrodynamics [12].

Figure 1(a) shows the schematic of the metamaterial slot waveguides. Two identical waveguides with square cross sections (both width w and height h are equal to 80 nm) are closely placed with a nanoscale gap g along the y direction. In each waveguide, the hyperbolic metamaterial is constructed with alternative thin layers of silver (Ag) and germanium (Ge). The multilayer metamaterial can be treated as a homogeneous effective medium and the principle components of the permittivity tensor are determined from the effective medium theory (EMT) [13],

$$\varepsilon_x = \varepsilon_z = f_m \varepsilon_m + (1 - f_m)\varepsilon_d,$$
$$\varepsilon_y = \frac{\varepsilon_m \varepsilon_d}{f_m \varepsilon_d + (1 - f_m)\varepsilon_m}, \tag{1}$$

where f_m is the volume filling ratio of silver, and ε_d and ε_m are the permittivity of germanium and silver, respectively. $\varepsilon_d = 16$, and $\varepsilon_m(\omega) = \varepsilon_\infty - \omega_p^2/(\omega^2 + i\omega\gamma)$ from the Drude model, with a background dielectric constant $\varepsilon_\infty = 5$, plasma frequency $\omega_p = 1.38 \times 10^{16}$ rad/s, and collision frequency $\gamma = 5.07 \times 10^{13}$ rad/s.

Figure 2(a) shows the mode profiles of the metamaterial slot waveguides for the filling ratio $f_m = 0.4$, and the gap size $g = 10$ nm, calculated by the finite-element method (FEM) with COMSOL. A considerable enhancement of electric field E_y is observed at the slot region as a result of the abrupt change of ε_y at the metamaterial–air interface. Consequently, a large fraction of optical power flow is localized in the slot region, as clearly shown from the profile of optical power flow density S_z in Fig. 2(a). The gap size g plays a critical role in the optical field enhancement. Figure 2(b) gives a comparison of E_y field
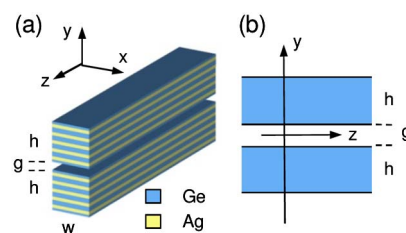

Fig. 1. (Color online) Schematic of the metamaterial slot waveguides. (a) Three-dimensional (3D) silver-germanium multilayer structures, and (b) approximated two-dimensional (2D) slab structures for theoretical analysis.

distributions for $g = 10$ nm and $g = 5$ nm. It is clear that a smaller gap size will lead to a stronger waveguide coupling and a larger electric field enhancement.

In order to understand the mechanism of electric field enhancement, theoretical analysis is conducted based on the two-dimensional (2D) coupled slab waveguides shown in Fig. 1(b), which is approximated from the three-dimensional (3D) coupled waveguides due to the negligible dependence of mode profiles on the x coordinate in Fig. 2(a). Assuming the optical field profiles of the slot waveguides have the form of $\exp(i\beta z - i\omega t)$, the coupled electric field can be expressed as follows:

$$E_y = E_0 \begin{cases} \cos\left(-k_y \frac{h}{2} + \varphi\right) \frac{\cosh(\gamma y)}{\cosh(\gamma \frac{g}{2})}, & 0 < |y| < \frac{g}{2}, \\ \frac{1}{\varepsilon_y} \cos\left[k_y\left(|y| - \frac{h+g}{2}\right) + \varphi\right], & \frac{g}{2} < |y| < \frac{g}{2} + h, \\ \cos\left(k_y \frac{h}{2} + \varphi\right) \exp\left[-\gamma\left(|y| - \frac{g}{2} - h\right)\right], & |y| > \frac{g}{2} + h, \end{cases} \quad (2)$$

where β is the mode propagation constant, ω is the angular frequency at $\lambda_0 = 1.55$ μm, and φ is the phase shift of optical field at the middle of each waveguide due to the waveguide coupling effect. The wave vector inside metamaterial k_y and the field decay rate in air γ are related to β through the following dispersion relations for hyperbolic metamaterial and air, respectively:

$$\frac{\beta^2}{\varepsilon_y} + \frac{k_y^2}{\varepsilon_z} = k_0^2, \qquad \beta^2 - \gamma^2 = k_0^2, \qquad (3)$$

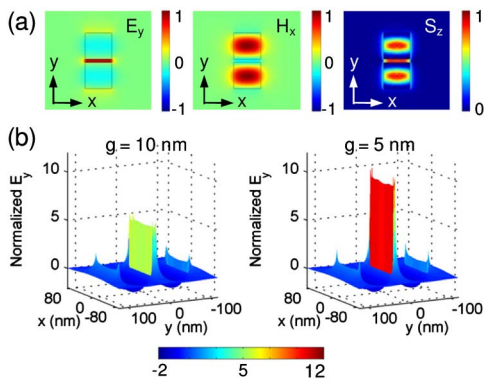where k_0 is the vacuum wave vector. By applying the continuity conditions of tangential field components

E_z and H_x at the metamaterial–air interface, the following characteristic equations are obtained:

$$\tan\left(-k_y \frac{h}{2} + \varphi\right) = -\frac{\gamma \varepsilon_z}{k_y} \tanh\left(\frac{\gamma g}{2}\right),$$

$$\tan\left(k_y \frac{h}{2} + \varphi\right) = \frac{\gamma \varepsilon_z}{k_y}. \qquad (4)$$

By solving the above equations, optical field properties can be obtained analytically, to reveal the mechanism of optical field enhancement.

Figures 3(a) and 3(b) present the effective refractive index along the propagation direction $n_{\text{eff},z} \equiv \beta/k_0$ of the metamaterial slot waveguides as a function of gap size g for two different filling ratios. The FEM simulation results of the 3D waveguides agree with the analytical results based on the 2D slab waveguides. Effective indices above 9 are obtained. As g decreases, the coupling between metamaterial waveguides is getting stronger so that both real($n_{\text{eff},z}$) and imag($n_{\text{eff},z}$) increase. The optical propagation length is calculated from $L_m \equiv 1/2\,\text{Im}(n_{\text{eff},z})k_0$. For $f_m = 0.4$, L_m will decrease from 509 nm at $g = 10$ nm to 487 nm at $g = 5$ nm.
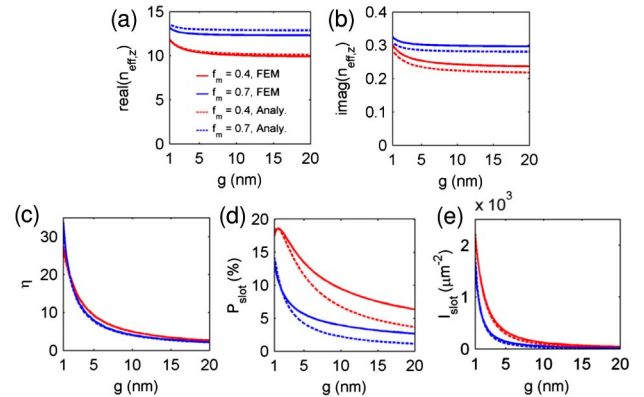
Fig. 3.   (Color online) (a) The real part of the effective refractive indices real($n_{\text{eff},z}$), (b) the imaginary part of the effective refractive indices and imag($n_{\text{eff},z}$), (c) electric field enhancement factor η, (d) optical power flow in the slot region P_{slot}, and (e) optical intensity in the slot region I_{slot} as a function of g for $f_m = 0.4$ and $f_m = 0.7$. Results from both FEM simulation and theoretical analysis are plotted.

Fig. 2.   (Color online) (a) Mode profiles of the metamaterial slot waveguide with $f_m = 0.4$ and $g = 10$ nm at $\lambda_0 = 1.55$ μm. (b) 3D surface plots of the E_y field distributions [normalized to $E_y(x = 0, |y| = |h + g/2|^+)$] for slot waveguides with $g = 10$ nm and $g = 5$ nm, respectively.

Due to the anisotropy of hyperbolic metamaterials, the optical mode profile of the metamaterial slot waveguide is distinguished from the case in a conventional dielectric waveguide. As noticed in Fig. 2(b), positive E_y in the slot region is accompanied with negative E_y inside waveguides. The electric field enhancement factor η is then defined as the ratio of the electric fields at the two boundaries of each waveguide, $\eta \equiv E_y[|y| = (g/2)^-/E_y[|y| = (g/2 + h)^+]$. As g is getting smaller, E_y field is enhanced greatly and η increases, as shown in Fig. 3(c). An analytical expression for η can be derived as

$$\eta \approx \sqrt{\frac{1 + \varepsilon_y|\varepsilon_z|}{1 + \varepsilon_y|\varepsilon_z|\tanh^2\left(\gamma\frac{g}{2}\right)}} \qquad (5)$$

in the condition of $k_y \gg k_0$ and $\gamma \gg k_0$. It is clear from Eq. (5) that η depends on g, γ, and permittivity tensor. For a higher f_m, both γ and $\varepsilon_y|\varepsilon_z|$ have larger values so that η will exhibit a larger growth rate as g decreases, as illustrated in Fig. 3(c). Although ε_y directly dominates the electric field discontinuity at the slot interfaces, ε_z will also affects the magnitude of electric field and therefore the field enhancement.

As a result of the electric field enhancement, optical power flow P_{slot} and averaged optical intensity $I_{\text{slot}} = P_{\text{slot}}/wg$ inside the slot region can also be enhanced dramatically. Figures 3(d) and 3(e) show the calculated P_{slot} and I_{slot} (normalized to the incident optical power flow) as a function of g for different filling ratios. As light can be strongly compressed in the nanoscale slot waveguide, optical intensity up to 2000 μm^{-2} is achieved in the slot region, which is more than 25 times stronger than that in a silicon slot waveguide (with a maximum of 80 μm^{-2} [1]). The analytical expression for P_{slot} and I_{slot} can be approximated as well:

$$P_{\text{slot}} \approx \frac{r_g}{1 + r_g}, \quad I_{\text{slot}} = \frac{P_{\text{slot}}}{wg} \approx \frac{1}{wg}\frac{r_g}{1 + r_g},$$

$$r_g \approx \frac{\varepsilon_y}{h}\frac{\frac{g}{2}\left[1 + \frac{\sinh(\gamma g)}{\gamma g}\right]}{1 + \varepsilon_y|\varepsilon_z|\sinh^2\left(\gamma\frac{g}{2}\right)}, \qquad (6)$$

where r_g is the ratio of optical power flow in the slot region to that inside two waveguides. The analytical results can give a clear explanation on the gap size dependence of P_{slot} and I_{slot} inside the slot region, which are related to γg.

In reality, metamaterial slot waveguides 80 nm in height can be constructed with eight pairs of Ag–Ge layers. Figure 4 plots the electric field E_y profiles along $x = 0$ for $g = 5$ nm with two filling ratios. In the slot region and the exterior surrounding air, the E_y profiles calculated from multilayer structures overlap with the EMT prediction. Inside the waveguide cores, E_y field will oscillate around, due to the coupling of gap plasmons between multilayers. However, the spatially homogenized E_y is still consistent with the EMT calculation. It should be noted that the actual collision frequency of silver will increase when its thickness is a few nanometers [14]. Germanium also has slight optical loss at 1.55 μm.
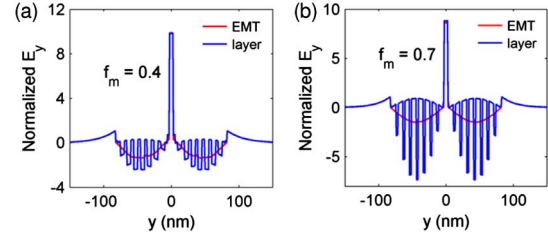

Fig. 4. (Color online) Comparison between the E_y field profiles along $x = 0$ for slot waveguides with (a) $f_m = 0.4$ and (b) $f_m = 0.7$, calculated from the EMT and realistic metal-dielectric multilayer structures (layer).

However, these increased material losses in real structures will not affect the optical field enhancement much, even though the propagation loss grows accordingly.

In conclusion, we have presented a new type of metamaterial slot waveguide for achieving giant electrical field enhancement. It is revealed that the optical field enhancement critically depends on gap sizes and anisotropic permittivity tensors. The demonstrated metamaterial slot waveguides with ultrahigh optical intensity will open up opportunities for many applications in enhanced light–matter interactions.

References

1. V. R. Almeida, Q. Xu, C. A. Barrios, and M. Lipson, Opt. Lett. **29**, 1209 (2004).
2. A. H. J. Yang, S. D. Moore, B. S. Schmidt, M. Klug, M. Lipson, and D. Erickson, Nature **457**, 71 (2009).
3. J. T. Shen, P. B. Catrysse, and S. Fan, Phys. Rev. Lett. **94**, 197401 (2005).
4. M. Choi, S. H. Lee, Y. Kim, S. B. Kang, J. Shin, M. H. Kwak, K.-Y. Kang, Y.-H. Lee, N. Park, and B. Min, Nature **470**, 369 (2011).
5. D. R. Smith and D. Schurig, Phys. Rev. Lett. **90**, 077405 (2003).
6. J. Yao, X. Yang, X. Yin, G. Bartal, and X. Zhang, Proc. Natl. Acad. Sci. **108**, 11327 (2011).
7. Z. Liu, H. Lee, Y. Xiong, C. Sun, and X. Zhang, Science **315**, 1686 (2007).
8. L. V. Alekseyev and E. Narimanov, Opt. Express **14**, 11184 (2006).
9. Y. J. Huang, W. T. Lu, and S. Sridhar, Phys. Rev. A **77**, 063836 (2008).
10. C. Koos, P. Vorreau, T. Vallaitis, P. Dumon, W. Bogaerts, R. Baets, B. Esembeson, I. Biaggio, T. Michinobu, F. Diederich, W. Freude, and J. Leuthold, Nat. Photon. **3**, 216 (2009).
11. M. Li, W. H. P. Pernice, and H. X. Tang, Nat. Photon. **3**, 464 (2009).
12. Q. Quan, I. Bulu, and M. Loncar, Phys. Rev. A **80**, 011810 (2009).
13. C. A. Foss, G. L. Hornyak, J. A. Stockert, and C. R. Martin, J. Phys. Chem. **98**, 2963 (1994).
14. W. Chen, M. D. Thoreson, S. Ishii, A. V. Kildishev, and V. M. Shalaev, Opt. Express **18**, 5124 (2010).